J Nanostruct 16(3): 3845-3860, Summer 2026

RESEARCH PAPER

Integrated 3D-Printed Microfluidic Lab-on-a-Chip for Multiplex Colorimetric Analysis of Human Urinary Biomarkers

Sarah T. Abdulkareem, Zaidon T. Al-aqbi *, Israa Qusay Falih*

Department of Chemistry, College of Science, University of Misan, Maysan, 62001, Iraq

ARTICLE INFO

Article History:
Received 22 March 2026
Accepted 20 June 2026
Published 01 July 2026

Keywords:
Biosensing
Colorimetric detection
Multiplex analysis
Point-of-care diagnostics
Urine biomarkers

ABSTRACT

The rapid, low-cost, and multiplexed detection of urine biomarkers is crucial for early disease diagnosis and regular clinical monitoring. These biomarkers collectively reflect key aspects of renal function, including glomerular filtration, tubular integrity, and metabolic alterations, thereby providing a comprehensive tool for the early detection of kidney dysfunction, particularly in high-risk conditions such as diabetes. In this study, we present a novel three-dimensional (3D) printed microfluidic device integrated with a colorimetric sensing platform for the simultaneous detection of multiple biomarkers in human urine samples. The proposed approach facilitates the quantitative assessment of ten clinically significant biomarkers: tyrosine, tryptophan, arginine, phenylalanine, cysteine, glucose, urea, creatinine, albumin, and uric acid. The microfluidic device was developed employing high-resolution 3D-printing technology for accurate channel design, reduced reagent usage and better portability. Specific colorimetric reactions were applied for each analyte, yielding specific optical responses that were recorded and analyzed by means of a digital imaging system. All the investigated biomarkers showed great sensitivity, good selectivity and satisfactory repeatability. Calibration curves were linear over physiologically relevant concentration ranges and had low limits of detection. Validation with real urine samples revealed good agreement with standard clinical laboratory tests proving the reliability and practical usability of the proposed device. In addition, the system enables quick analysis, little sample preparation and the opportunity for point-of-care testing. Overall, this work demonstrates the integration of 3D printing and microfluidic colorimetric sensing as an attractive strategy for the development of low-cost, portable and multiplexed diagnostic tools for clinical applications.

How to cite this article
Abdulkareem S., Al-aqbi Z., Qusay Falih I. Integrated 3D-Printed Microfluidic Lab-on-a-Chip for Multiplex Colorimetric Analysis of Human Urinary Biomarkers. J Nanostruct, 2026; 16(3):3845-3860. DOI: 10.22052/JNS.2026.03.071

INTRODUCTION

Chronic kidney disease (CKD) is defined as a gradual decline in kidney function lasting more than three months, leading to the accumulation of excess fluids and waste products in the body. If not properly managed from the early stages, it may progress to kidney failure. Kidney failure occurs when the kidneys lose their ability to adequately filter waste and excess fluid from the blood, resulting in their accumulation in the body.

* *Corresponding Author Email: zaidon.alaqbi@uomisan.edu.iq*

This work is licensed under the Creative Commons Attribution 4.0 International License.
To view a copy of this license, visit http://creativecommons.org/licenses/by/4.0/.

This condition may occur suddenly (acute kidney failure) or develop gradually (chronic kidney failure), and it becomes life-threatening if not properly treated [1-3].

The kidneys play a key role in maintaining the body's amino acid balance through synthesis, breakdown, filtration, reabsorption, and excretion of amino acids and peptides in urine. Approximately 50–70 g of amino acids is filtered daily, and about 97–98% are reabsorbed in the proximal tubules [4,5]. Renal amino acid metabolism supports gluconeogenesis, nitrogen removal, and acid–base regulation, and provides substrates for the citric acid and urea cycles; therefore, the kidneys are central to maintaining metabolic homeostasis [6,7].

Diabetic kidney disease is one of the leading causes of chronic kidney failure [8]. Patients with elevated protein levels in urine suffer from proteinuria, which is associated with many kidney disorders [9,10]. Urinary protein biomarkers are useful in diagnosing kidney and cardiovascular diseases, cancers, diabetes, and infections. Key biomarkers measured in blood or urine of kidney patients include creatinine, urea, uric acid, albumin, and the amino acids cysteine, tryptophan, phenylalanine, tyrosine, and arginine [11,12].

Several methods are used to detect these pathological markers in urine, including dipstick tests, quantitative proteinuria assays, and urinary proteomics. These rely on techniques such as chromatography, electrophoresis, and mass spectrometry to identify proteins associated with kidney diseases. Mass spectrometry and immunoassays are used to detect low-molecular-weight proteins, while GC-MS and fluorescence-based chromatography provide sensitive and accurate analysis [11,12].

Gas chromatography–mass spectrometry (GC-MS) is a powerful modern technique for urine analysis, combining separation of compounds by gas chromatography with accurate identification by mass spectrometry. It enables detection of amino acids, organic acids, ketones, and other metabolic products in urine, even at trace levels [13,14].

Urine analysis by GC-MS involves sample collection and preparation by removing proteins and impurities, chemical derivatization of non-volatile compounds, separation by gas chromatography, and identification by mass spectrometry using reference databases. This method allows detection of abnormal amino acids related to kidney disorders, investigation of metabolic disturbances in diabetes and renal failure, and monitoring of chronic kidney disease progression. It also supports the discovery of new biomarkers for early diagnosis and prediction of complications [15,16].

Despite its advantages, GC-MS has limitations. It is mainly suitable for volatile compounds or those that can be made volatile, so non-volatile substances require complex preparation. Sample preparation is time-consuming and often involves derivatization. In addition, the instruments are expensive, and their operation and data interpretation require high technical skill [17].

Liquid-phase chromatography (LPC/HPLC) is another important method for separating biological compounds in urine, such as amino acids, hormones, and metabolic by-products. It provides accurate quantitative measurements, supports diagnosis of metabolic disorders, and helps monitor kidney and liver function. LPC can handle complex samples without degradation and allows simultaneous analysis of multiple compounds [18,19]. It is also widely used for drug and toxin detection in medical and forensic fields. However, HPLC is limited to compounds soluble in the selected solvents, and sample preparation may be complex and require chemical derivatization. The equipment is costly and requires skilled operation to ensure reliable results [20,21].

Several devices are widely used in medical laboratories, UV–Vis spectrophotometers. These instruments are employed for UV-Vis spectroscopy in research, production and quality control to classify and analyze materials. UV-Vis spectroscopy is based on the absorption of light by a sample. Important information, such as sample purity, can be determined from the amount and wavelength of light absorbed. Additionally, the amount of light absorbed is proportional to the sample concentration, enabling quantitative spectroscopic analysis [22,23].

In recent years, microfluidic technologies emerged as a potential alternative to traditional analytical methods for biomarker detection in human urine, driven by the demand for quick, sensitive, and point-of-care diagnostic instruments. Conventional methods, including spectrophotometry, chromatography, and immunoassays, while highly precise and

CC BY

established, frequently necessitate advanced instrumentation, substantial sample volumes, extensive sample preparation, and skilled personnel, thereby constraining their use in decentralized or resource-constrained environments. Conversely, microfluidic systems provide substantial benefits, such as downsizing, diminished reagent and sample usage, expedited analysis duration, and the capacity to amalgamate several analytical procedures within a singular device [24,25]. These technologies provide exact regulation of fluid dynamics and response parameters at the microscale, improving analytical efficacy and consistency. Moreover, recent advancements in fabrication methods, especially 3D printing have enabled the formation of affordable, customizable, and portable microfluidic devices appropriate for multiplexed biomarker detection [26]. Microfluidics, when integrated with colorimetric sensing, facilitates uncomplicated signal detection without requiring intricate instrumentation, rendering it exceptionally appealing for point-of-care applications. Consequently, microfluidic-based methodologies are progressively embraced as effective and scalable substitutes for conventional laboratory techniques in urinary biomarker analysis, possessing significant potential to revolutionize clinical diagnostics and personalized healthcare [27,28].

Here, we present a novel 3D-printed microfluidic device featuring ten circular channels and an integrated detection area for the colorimetric detection of amino acids, proteins, and other metabolites present in human urine samples.

MATERIALS AND METHODS

Chemicals

Tryptophan ($C_{11}H_{12}N_2O_2$), tyrosine ($C_9H_{11}NO_3$), albumin (a complex protein), arginine ($C_6H_{14}N_4O_2$), cysteine ($C_3H_7NO_2S$), phenylalanine ($C_9H_{11}NO_2$), alpha-naphthol ($C_{10}H_8O$), creatinine ($C_4H_7N_3O$), and ammonium citrate ($(NH_4)_3C_6H_5O_7$) were supplied by Sigma-Aldrich. Strong acids and solvents such as sulfuric acid (H_2SO_4), hydrochloric acid (HCl), nitric acid (HNO_3), glacial acetic acid (CH_3COOH), ethanol (C_2H_5OH), sodium hydroxide (NaOH), and sodium hypochlorite (NaOCl) were purchased from Merck. While ammonia (NH_3), sodium chloride (NaCl), mercuric nitrate ($Hg(NO_3)_2$), potassium chloride (KCl), magnesium sulfate ($MgSO_4$), potassium bicarbonate ($KHCO_3$), Sodium Nitroprusside ($Na_2[Fe(CN)_5NO]$), potassium hydrogen phosphate (KH_2PO_4), and potassium hydrogen sulfate ($KHSO_4$) were purchased from Luba Chemie. pH 4.01, 7.01 and 10.01 Technical Calibration Solutions with Electrode Storage Solution and Cleaning Solution. *Boswella sacr*a and distill water. Ready-made reagents, including urea and glucose kits, were purchased from Bio Research, while creatinine and uric acid kits were obtained from Spinreact.

Sample Preparation

Reagents for colorimetric detection of target biomarkers were made using the following reagents and techniques. The Hopkins–Cole reagent for the detection of tryptophan was created by the use of glyoxylic acid generated by exposing glacial acetic acid to sunlight under 10 days, together with concentrated sulphuric acid. Tyrosine was tested under Millon's test using a 15% (w/v) solution of mercuric nitrate in 15% (v/v) nitric acid. Detection of arginine was done by the Sakaguchi reaction. For this, 0.5 g of α-naphthol was dissolved in 50 mL of ethanol. A 40% solution of sodium hydroxide was prepared by dissolving 10 g in 25 mL of distilled water. Both solutions were stored in opaque glass containers. An additional reagent, commercially available 5.25% solution of sodium hypochlorite, was used. For the examination of cysteine, 1 g potassium cyanide was dissolved in 20 mL distilled water in a volumetric flask. Separately, 1 g sodium nitroprusside was dissolved in 20 mL distilled water. The albumin detection reagent (copper nanoparticle CuNPs) was prepared according to our previously published work [24], by combining 10 mL of 0.1 M copper sulphate solution, 16 mL of 0.1 M sodium hydroxide, and 16 mL of 10% *Boswellia sacra* and heating at 60–70 °C with constant stirring; after 5 min, hydrazine hydrate was added and the mixture was heated further for 30 min after a dark red colour was observed within 4 min. The combination was then centrifuged at 6000 rpm for 30 min and the filtrate separated and kept in an opaque volumetric flask for further use. Finally, a 15% ferric chloride solution was produced for the detection of phenylalanine and stored in an opaque glass bottle to preserve its stability.

Human urine samples from a healthy volunteer and patients with CKD were obtained in accordance with the guidelines established by the University of Misan / College of Science / Department of Chemistry, Ethics Committee,

CC BY

University of Misan (Ethics Approval Ref D.A. 132 dated 9-Aug-2025) and were subsequently spiked with various biomarkers.

Instrumentation

The HI pH-211 is an advanced innovation-focused instrument designed with high-quality engineering, making it suitable for both industrial use and quality control laboratories. It is capable of measuring millivolts on two ranges ±399.9 mV and ±1999 mV and works in combination with ISE and ORP electrodes.The device includes several smart features aimed at minimizing calibration mistakes and making operation easier offering clear guidance through an organized and user-friendly display.

The Shimadzu UV-1800 is a compact, double-beam UV-Visible spectrophotometer engineered for accurate and reliable measurements. It provides a spectral resolution of 1nm, meeting the standards of both the European and Japanese Pharmacopoeias. Its space-saving design (450 × 490 mm) makes it well suited for laboratories with limited bench space. The instrument supports various measurement functions, including photometric analysis, kinetic measurements and multi-component analysis. With UV Probe software, users can control the system entirely through a PC and easily export data using a USB drive. It is widely used in scientific research, protein assays, DNA analysis and many other laboratory applications.

The UV–Vis spectrophotometer (Shimadzu, Japan) was used to record the observed Localized Surface Plasmon Resonance (LSPR) band for the red-brown CuNPs solution, which was one of the techniques to diagnose the synthesised CuNPs@BS nanosensors. The crystallinity of CuNPs@BS was investigated by X-ray diffraction (XRD) of the materials utilizing PAN analytical X'PERT PRO model X-ray diffractometer at 30 kV and 45 mA. The instrument was operated in a 2θ geometry

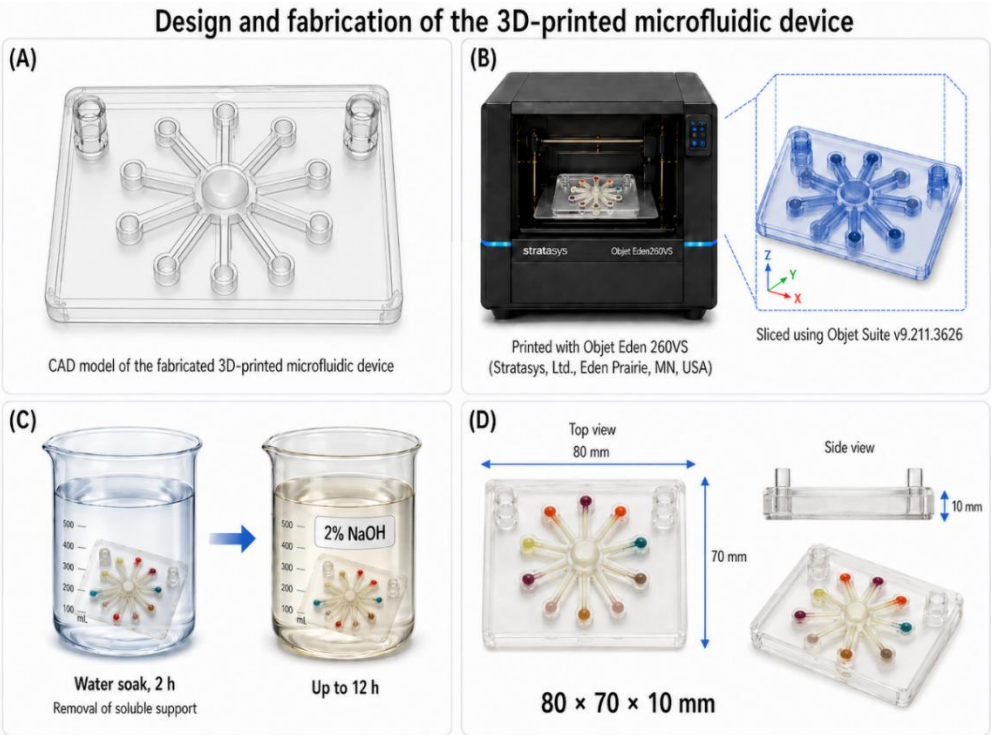

Fig. 1. Design, production, post-processing and dimensional characterization of the 3D-printed microfluidic device. (A) CAD drawing of the microfluidic device illustrating the central chamber, standard radial microchannels, terminal reservoirs, and inlet/outlet ports. (B) Fabrication workflow with the Objet Eden 260VS 3D printer, where the model of the device was sliced with Objet Suite v9.211.3626. (C) Device after printing, soaked in water for 2 hours to remove soluble support material, then immersed in 2% NaOH for up to 12 hours. (D) Final device: Photographic and dimensional presentation, including total dimensions of 80 x 70 x 10 mm.

CC BY

using CuKα (λ = 1.540 Å) radiation. The scanning rate was 0.026/min over the range of 0◦ to 80◦. The CuNPs@BS was also examined by high resolution transmission electron microscopy (HR-TEM) using a JEOL instrument (model 1200 EX; Cu grid) at an accelerating voltage of 40 kV with a ZEISS-TEM instrument at magnification of 200 and field emission scanning electron microscopy (FESEM) at an accelerating voltage of 20 kV (Tescan MIRA3 FEG-EDAX).

Fabrication of Microfluidic Device

The 3D printed microfluidic device was designed and constructed using SolidWorks software 2022 and then fabricated using the Objet Eden 260VS professional 3D printer (Stratasys, Ltd., Eden Prairie, MN, USA). Models were sliced and processed for printing using Objet Suite v9.211.3626 (Stratasys Ltd., Eden Prairie, MN, USA) according to the printer manufacturer's instructions.

The 3D-printed microfluidic device was soaked in water for two hours to remove the soluble support, then put in 2% NaOH for up to twelve hours. The overall dimensions of the 3D-printed item were 80 x 70 x 10 mm as illustrated in Fig. 1.

The photographs of the 3D printed devices were photographed using the main camera of an iPhone 13 Pro Max smartphone. The colour intensity was measured using ImageJ software. Colour intensity images were converted to greyscale to standardize. Then the background was subtracted and the average grey value was determined.

Microfluidic Device Operation

The 80 x 70 x 10 mm 3D-printed microfluidic device was uniquely designed to simultaneously detect numerous biomarkers. The whole image of the microfluidic device is shown in Fig. 2. As we have mentioned before in our research [25-29], it is quite easy to introduce both reagent and sample components into the reservoir with an autopipette, thus we have opted for this design of the reservoirs with the reagent and sample components. The developing colour is inspected after the material is injected. The data is processed and the quantification step is done using ImageJ software.

Optimization the optimum conditions

Biomarkers such as tyrosine, tryptophan, arginine, phenylalanine, cysteine, glucose, urea, creatinine, albumin, and uric acid are key indicators of the overall health status of individuals with chronic kidney disease. To determine the optimal conditions for assessing these biomarkers, they are measured using precise medical or laboratory instruments to ensure accurate and reliable readings. The obtained values are then compared with medically established reference ranges for healthy individuals, which define the normal limits for each biomarker.

The determination of optimal conditions involves repeating the measurements multiple times under varying experimental conditions,

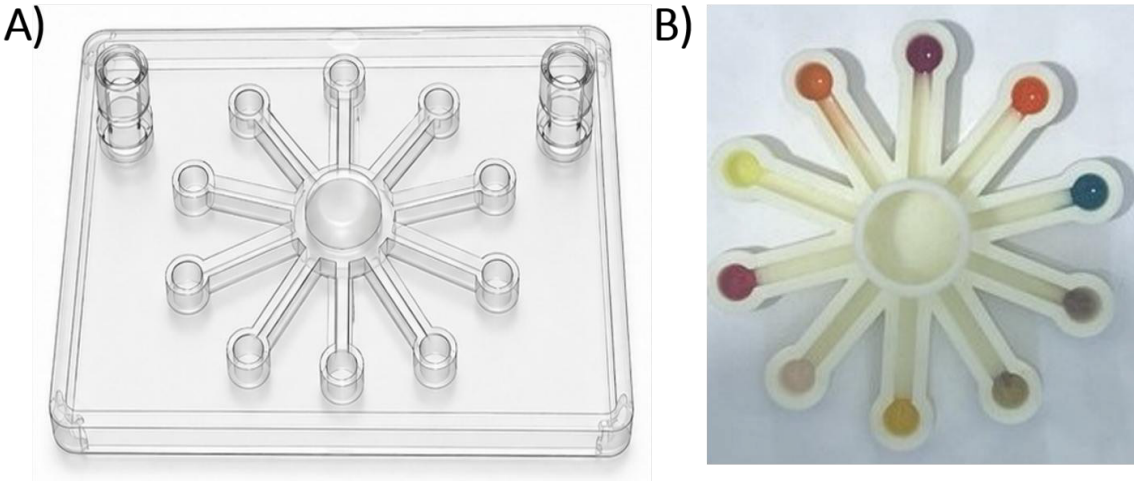

Fig. 2. AutoCAD model (A) and photo (B) of the microfluidic device 3D printed. The CAD model shows the design of the central hub with radial channels moving to the circular reservoirs for analyte analysis. The device is made using 3D printing and is proposed for accurate fluidic applications.

CC BY

taking into account factors such as time, pH, temperature, and potential interferences. The results are then subjected to statistical analysis to identify the values that best represent optimal physiological conditions. Values that fall within the normal range indicate stable bodily functions. These values can be used as reference benchmarks for evaluating health status and for the early detection of potential disorders.

Time

The absorbance of each of the previously mentioned vital signs was measured, at different time intervals ranging from 1 minute to 120 minutes, and at various rates as described in the results section.

pH (acidity)

The absorption of the aforementioned biomarkers was measured using spectrophotometers, at different pH values as mentioned in the results, and the absorption value for each pH level was recorded, with the aim of determining the optimal pH level for each reagent.

Temperature

The absorption of the above biomarkers was measured using spectrophotometers, at different temperatures (20-60) °C and at a constant rate of 5°C, and the absorption value for each specific temperature was recorded, with the aim of determining the optimal temperature for each reagent.

Interferences

This test is conducted to determine whether interfering ions are present that may affect the action of the reagents used for the previously mentioned vital signs. This is assessed by observing any color change that occurs when these ions are added to the reagents employed for the detection of each vital sign. The most important of these ions Na^{+},Cl^{-},Mn^{+2},Cu^{+2},Hg^{+2},Li^{+},CO_3^{2-},Zn^{+2},Pb^{+2},K^{+},PO_4^{-3}.

Statistical Analysis

Group comparisons utilized Student's t-test and Tukey's post hoc test, whilst one-way analysis

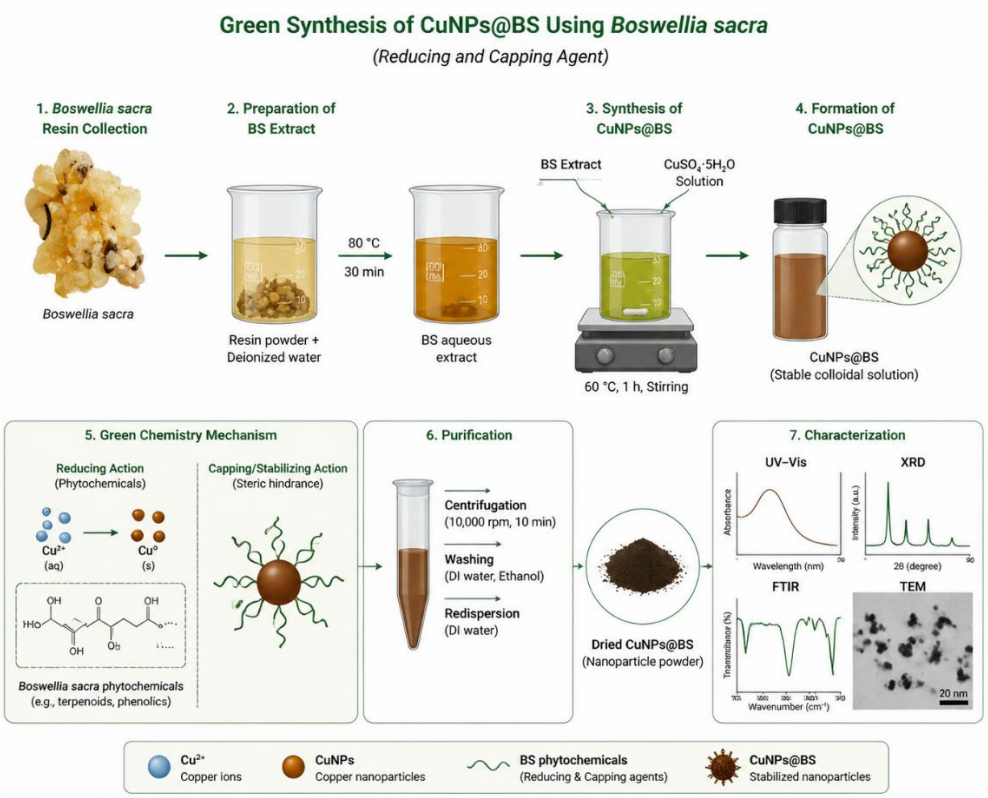

Fig. 3. Green synthesis, purification, characterization, and proposed formation mechanism of CuNPs@BS using *Boswellia sacra* extract as the reducing and capping agent.

CC BY

of variance (ANOVA) was employed to assess statistically significant differences among different groups. All measurementswere performed in triplicate, and the findings are shown as mean ± standard deviation (SD). The standard error of the mean (SEM) was computed from the three independent replicates to represent data variability. Statistical analyses were conducted utilizing Microsoft Excel 2016 (Microsoft Corp., USA).

RESULTS AND DISCUSSION

Fabrication of CuNPs@BS for Albumin Detection

Nanotechnology is an emerging field that involves the production of nanoparticles via simple, inexpensive, environmentally and friendly techniques, using green natural resources. In recent years, various green metallic nanoparticles including silver, copper, titanium and selenium based on the technique of green reduction involving active biological components in plants have been synthesized. Polysaccharides, proteins, glycosides, carboxylic acids, flavonoids, hydration compounds and a certain number of metals are important substances in the plant [30]. *Boswellia sacra* is of significant bio-significance and hence several research organizations have investigated the contents of *Boswellia sacra*. The reducing agents 3-O-acetyl-11-keto-β-boswellic acid, acetyl-β-boswellic acid and β-boswellic acid are found in *Boswellia sacra* [31]. According to another study done using High-Performance Liquid Chromatography (HPLC) analysis [32], it contains important active compounds from boswellic acids and polysaccharides like arabinose, xylose, and galactose. Thus, CuNPs was prepared using the reducing power of the *Boswellia sacra* extract. *Boswellia sacra* extract contains reducing groups with high value. This is due to boswellic acids and monosaccharides. The structure of these groups is identified as hydroxy-flavonoid with high hydroxyl groups ratio.

The structure is essential when metal ions are reduced to nanoparticles. Consequently, the boswellic acids and monosaccharides facilitate the synthesis of CuNPs@BS (Fig. 3). Numerous published research have verified the notion that plant extracts can lower various metal ions, including Zn^{2+}, Cu^{2+}, Fe^{3+}, Ti^{4+}, and Se^{2+} [24,33].

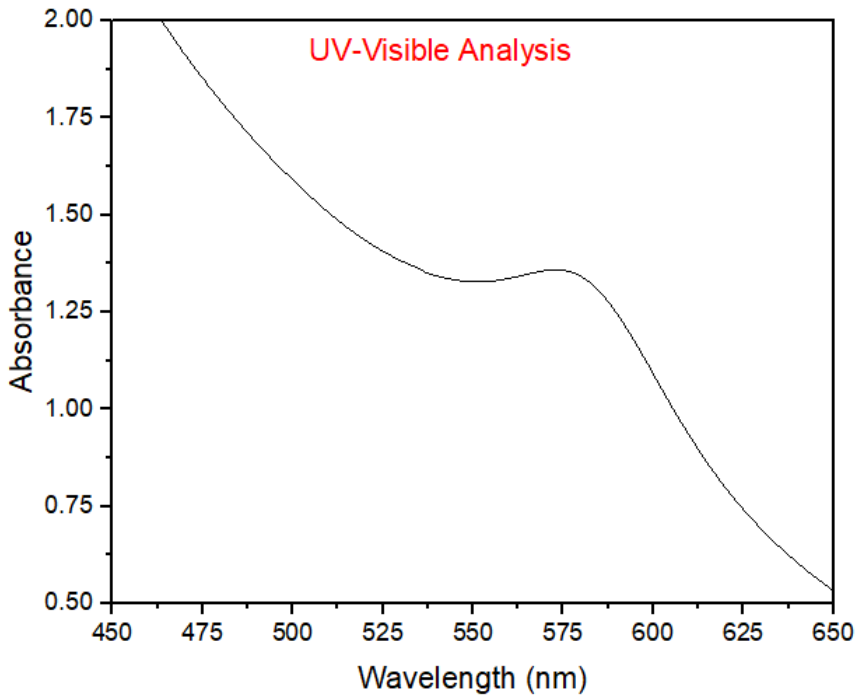

Fig. 4. The UV–visible absorption spectrum of copper nanoparticles (CuNPs) demonstrates the distinctive surface plasmon resonance (SPR) band, which validates nanoparticle production and elucidates their optical characteristics, size distribution, and colloidal stability.

CC BY

Characterization of CuNPs@BS

The effective green synthesis of CuNPs@BS was validated using UV–Visible spectroscopy, X-ray diffraction (XRD), field emission scanning electron microscopy (FESEM), transmission electron microscopy (TEM), and zeta potential analysis. These techniques offer supplementary insights into optical response, crystalline structure, shape, particle size, and colloidal stability, which are crucial for confirming the synthesis of metal nanoparticles designed for sensing applications. The utilization of *Boswellia sacra* extract is especially beneficial due to the resin's bioactive phytochemicals, comprising boswellic acid derivatives and terpenoid components, which can facilitate the reduction of Cu^{2+} ions and the subsequent stability of the nanoparticle surface [34].

The UV–Visible spectra of CuNPs@BS displayed a characteristic absorption band at about 580 nm, indicating the creation of copper nanoparticles due to surface plasmon resonance and/or interband electronic transitions. Previous investigations have shown that copper nanoparticles frequently exhibit an optical absorption band in the visible region, usually about 560–575 nm, which is affected by particle size, shape, oxidation state and the surrounding capping environment. The creation of this band along with the observed shift of colour from blue to red-brown confirms the reduction of copper ions and formation of CuNPs@BS. The broadness of the absorption peak can be due to the polydispersity of the nanoparticles and the presence of *Boswellia sacra* derived phytochemicals on the surface of the nanoparticles. The importance of such organic molecules attached to the surface is that they increase water dispersibility and give functional groups for interaction with albumin in the detection process [35], as shown in Fig. 4.

Crystalline structure of the produced CuNPs@BS was analyzed by X-ray diffraction (XRD) analysis.

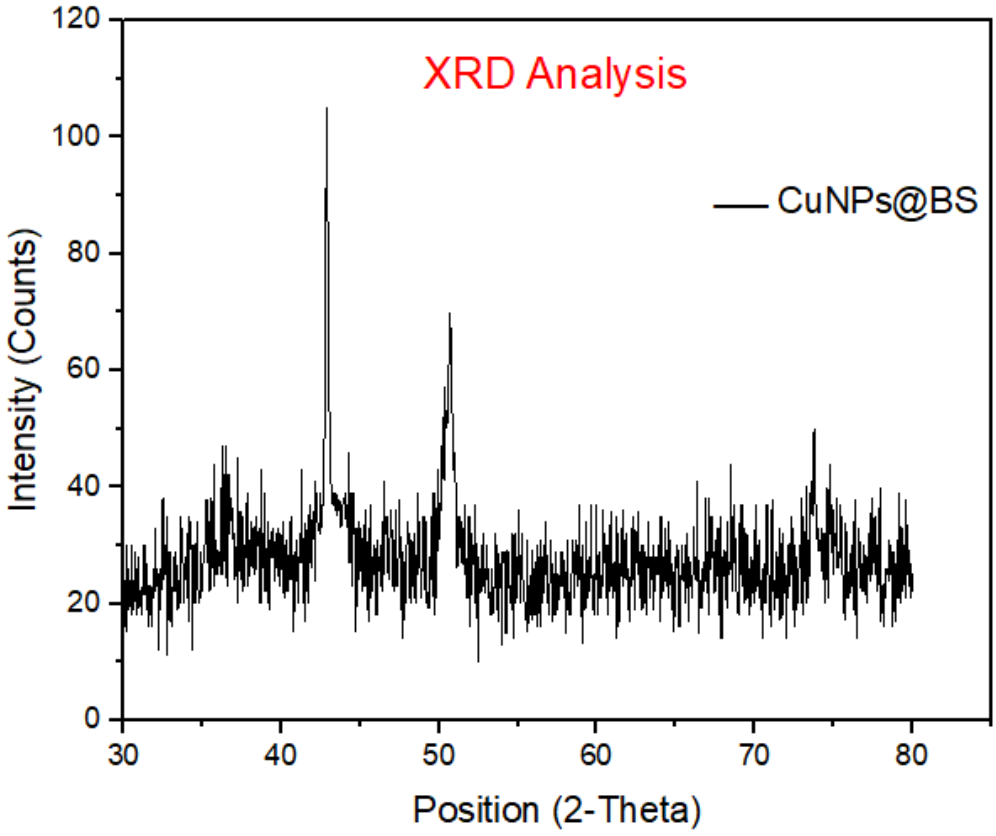

Fig. 5. X-ray diffraction (XRD) pattern of copper nanoparticles (CuNPs), exhibiting the distinctive diffraction peaks associated with crystalline copper phases. The peak positions and intensities validate the successful synthesis, crystallinity, and phase purity of the nanoparticles.

CC BY

The diffraction peaks at 2θ are ascribed to the crystalline planes of CuNPs@BS. Metallic copper nanoparticles have peaks generally observed at 42.8°, 50.6° and 73.7° corresponding to the (111), (200) and (220) planes of face-centered cubic copper respectively. The comparatively broad diffraction peaks indicate the production of nanoscale crystallites, which could be due to restricted growth of copper nuclei in the presence of *Boswellia sacra* proteins. If present, the weak extra peaks corresponding to copper oxides can be explained by partial surface oxidation of CuNPs. This is often encountered since copper nanoparticles are particularly vulnerable to oxidation under ambient circumstances [36]. However, the phytochemical residues of *Boswellia sacra* can operate as a protective capping layer that limits the excessive aggregation and improves the structural stability as shown in Fig. 5.

The production of CuNPs@BS was further validated by FESEM analysis providing an insight into the surface shape of the dried nanoparticle material. FESEM micrographs indicated spherical particles with moderate aggregation. In the case of dry nanoparticle samples, such an aggregation is expected, since solvent evaporation and capillary forces can lead to the close contact of the particles during the sample preparation. Thus, FESEM should be seen as a proof of surface morphology and dispersion of particles rather than a single proof of the colloidal particle size. However, TEM offers more direct visualization of the main nanoparticles. TEM pictures demonstrate that the average size of the particles is in the range of ~35 nm, confirming that the produced CuNPs@BS are in the nanoscale range. The disparity between FESEM- and TEM-derived dimensions may be due to the aggregation of particles in the dry condition, variances in imaging resolution [37], and the difference between primary particle size and secondary aggregates as shown in Fig. 6.

TEM study also shows the stabilizing action of *Boswellia sacra* extract. The particles seemed to be well dispersed and the slight organic layer surrounding the particles may be due to surface capping by phytochemical components from the extract. The capping layer is important for the detection of albumin because it provides a biologically compatible interface with functional groups such as hydroxyl, carbonyl, and carboxylate moieties that can interact with albumin molecules through hydrogen bonding, electrostatic interactions, or surface adsorption. These interactions might change the local refractive index, aggregation state or surface charge of CuNPs@BS, resulting in detectable optical or physicochemical alterations for the detection of albumin [38].

The zeta potential study was performed to define the colloidal stability and surface charge of CuNPs@BS. The zeta potential measurement value (− 31 mV) shows that the nanoparticles are negatively charged on their surface. Generally, zeta potential values ±35 mV are often considered to indicate electrostatically stable nanoparticle dispersions, whereas lower absolute values may indicate moderate stability or a tendency toward aggregation. . However, this interpretation is highly dependent on pH, ionic strength, solvent composition, and the electrokinetic model

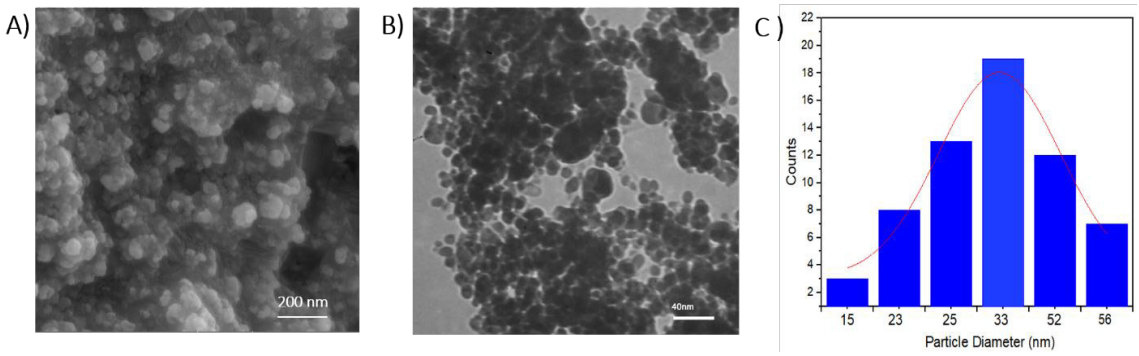

Fig. 6. Morphological and size analysis of copper nanoparticles (CuNPs): (A) FESEM image of the synthesized nanoparticles, showing the surface morphology and distribution; (B) TEM image showing the shape and nanoscale structure of the particles; (C) particle size distribution histogram from TEM analysis, showing average particle diameter and size dispersion.

CC BY

used. The negative charge detected could be due to ionizable functional groups of *Boswellia sacra* phytochemicals adsorbed on the surface of nanoparticles [39]. This surface charge is important for colloidal dispersion stability, and is also essential to albumin sensing, since albumin adsorption can lead to quantifiable changes in nanoparticle charge, dispersion state, or optical response as shown in Fig. 7.

The comprehensive characterization results validate the synthesis of CuNPs@BS via a green method utilizing *Boswellia sacra* as both the reducing and capping agent. UV–Visible spectroscopy proved nanoparticle production, XRD revealed crystalline structure, FESEM and TEM validated nanoscale morphology, and zeta potential studies indicated colloidal stability. The physicochemical features affirm the appropriateness of CuNPs@BS as a functional nanomaterial for albumin detection, since the phytochemical-capped copper nanoparticle surface enhances interaction with albumin, yielding a measurable analytical response.

Factors Influencing the Sensing Process

Effect of pH

The pH of the reaction system was measured to accurately determine and adjust the medium to target values. To achieve this, the pH was adjusted using dilute solutions of hydrochloric acid and sodium hydroxide. The study also included evaluating the response of a range of biomarkers, including albumin, tyrosine, cysteine, tryptophan, phenylalanine, arginine, urea, uric acid, glucose, and creatinine. Supporting Information shows that pH changes significantly affect the absorbance values of all studied biomarkers. The optimal pH value that achieves the highest absorbance was identified adopted to ensure the reliability and accuracy of the analytical measurements.

Effect of Time

The colorimetric and absorbance responses of the reactive system were monitored after the addition of the reagent using a microfluidic

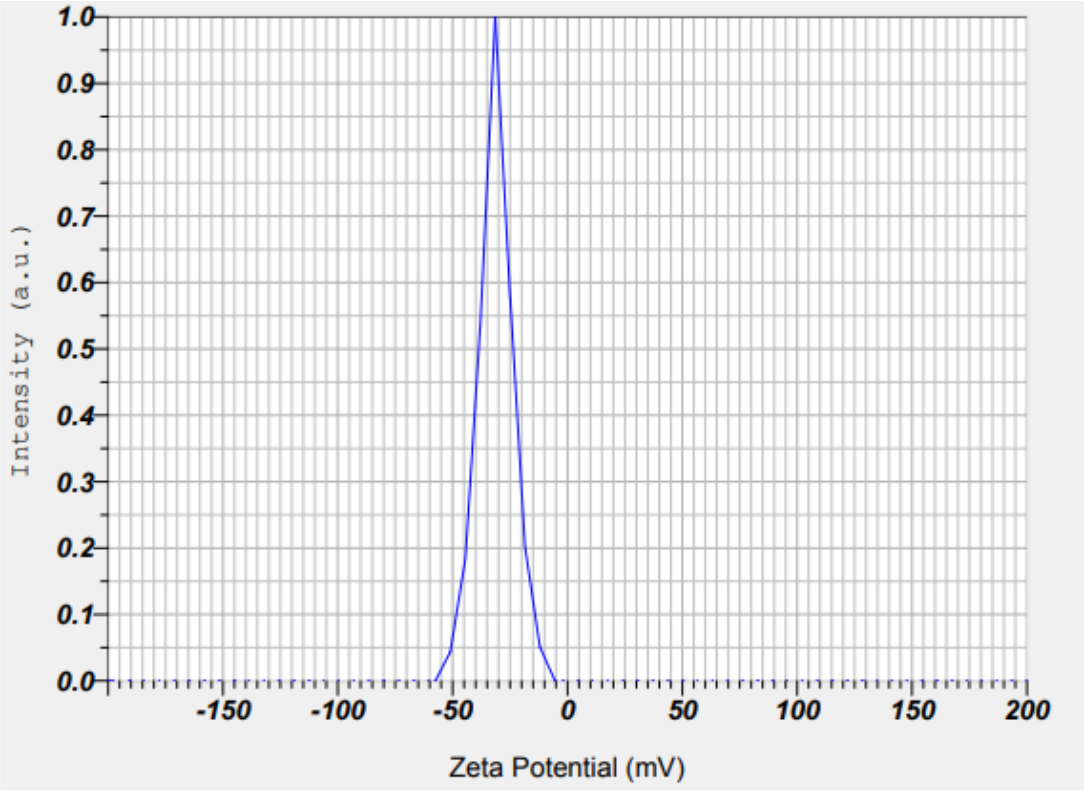

Fig. 7. Zeta potential of produced CuNPs. The surface charge of CuNPs was -31 mV demonstrating good colloidal stability with good electrostatic repulsion between particles.

device at predetermined time intervals. The study included the following biomarkers: albumin, tyrosine, cysteine, tryptophan, phenylalanine, arginine, urea, uric acid, glucose, and creatinine. Supporting Information showed that the absorbance values changed with time after the reaction began, with a stable response observed within a short period, followed by a steady-state phase with no significant changes. Therefore, a specific reaction time was adopted for subsequent experiments due to the stability of the response and the reproducibility of the measurements. Overall, the lab-on-a-chip system demonstrated adequate stability, enabling efficient and reliable measurements.

Effect of Temperature

The absorbance response of the reactive system was monitored for the same sample at different temperatures ranging from 20 to 60 °C, with a 5°C increment per step, using gradual heating and cooling. The study included the following biomarkers: albumin, tyrosine, cysteine, tryptophan, phenylalanine, arginine, urea, uric acid, glucose, and creatinine. Supporting Information showed variations in absorbance values with temperature changes, and the temperature range that yielded a stable and reliable response from the system was identified, enabling measurements to be taken under precise and controlled conditions.

Effect of Interferences

The existence of potential interfering species is a crucial element influencing the precision and dependability of colorimetric detection techniques for urinary biomarkers, especially in intricate biological matrices like human urine. Urine has several inorganic ions and organic chemicals that can affect analytical data via chemical interactions, competitive reactions, or matrix effects. This study systematically evaluated the interference behaviour of common ions, including Na^+, K^+, Li^+, Cl^-, CO_3^{2-}, PO_4^{3-}, and transition/heavy metal ions such as Mn^{2+}, Cu^{2+}, Zn^{2+}, Pb^{2+}, and Hg^{2+}, in relation to the detection of multiple biomarkers: tyrosine, tryptophan, arginine, phenylalanine, cysteine, glucose, urea, creatinine, albumin, and uric acid. The results indicated that these ions did not cause substantial interference with the colorimetric responses of the targeted analytes under the optimum experimental circumstances, signifying a high level of selectivity of the proposed sensing system.

This low interference is due to the selectivity of the utilized chemical processes, wherein each biomarker engages in a unique and selective reaction pathway that is mostly unaffected by the presence of concurrent ions. For example, reactions like the Hopkins–Cole test, Millon's test, and Sakaguchi reaction depend on interactions specific to functional groups (e.g., indole, phenolic, and guanidine groups), which cannot

Table 1. Assessment of potential interference from common inorganic ions (Na^+, K^+, Li^+, Cl^-, CO_3^{2-}, PO_4^{3-}, Mn^{2+}, Cu^{2+}, Zn^{2+}, Pb^{2+}, and Hg^{2+}) on the colorimetric detection of specific urinary biomarkers (tyrosine, tryptophan, arginine, phenylalanine, cysteine, glucose, urea, creatinine, albumin, and uric acid), illustrating the selectivity and anti-interference efficacy of the proposed microfluidic sensing platform.

Interferences	Tyrosine	tryptophan	Uric acid	Urea	Phenylalanine	Glucose	Cysteine	Creatinine	Albumin	Arginine
Na^+	–	–	–	–	–	–	–	–	–	–
Cl^-	–	–	–	–	–	–	–	–	–	–
Mn^{+2}	–	–	–	–	–	–	–	–	–	–
Cu^{+2}	–	–	–	–	–	–	–	–	–	–
Hg^{+2}	–	–	–	–	–	–	–	–	–	–
Li^+	–	–	–	–	–	–	–	–	–	–
CO_3^{-2}	–	–	–	–	–	–	–	–	–	–
Zn^{+2}	–	–	–	–	–	–	–	–	–	–
Pb^{+2}	–	–	–	–	–	–	–	–	–	–
K^+	–	–	–	–	–	–	–	–	–	–
PO_4^{-3}	–	–	–	–	–	–	–	–	–	–

CC BY

be easily replicated or interfered with by basic inorganic ions. The microfluidic technology improves selectivity by regulating reaction conditions, minimizing diffusion effects, and decreasing nonspecific interactions. The lack of interference from prevalent urine ions like sodium and potassium is crucial due to their elevated physiological levels, while the absence of influence from transition and heavy metal ions indicates resilience against possible contamination or pathological fluctuations.

Moreover, the stability of the colorimetric signals in the presence of these ions demonstrates that the system is resilient to fluctuations in ionic strength and does not experience substantial signal suppression or enhancement. This is a significant advantage for practical applications, given that urine composition can fluctuate considerably among persons and physiological states. The findings affirm that the engineered 3D-printed microfluidic colorimetric device exhibits robust anti-interference capabilities, rendering it appropriate for precise, dependable, and multiplexed detection of urinary biomarkers in real sample analysis without extensive sample pretreatment. **Table 1 summaries** the selectivity results.

Detection of Multiple Biomarkers in Artificial Urine

This study examined the spiked concentrations of different urinary biomarkers (tyrosine, tryptophan, arginine, phenylalanine, cysteine, glucose, urea, creatinine, albumin, and uric acid) with a colorimetric detection method in synthetic urine. The primary aim of the spiking recovery investigation was to evaluate the precision of the detection method by juxtaposing the known concentrations of the spiked biomarkers with the observed values. The elevated recovery rates for all biomarkers indicate that the assay accurately measures the introduced chemicals, with negligible matrix interference. Recovery rates of 90-110% generally signify a procedure that is both precise and dependable, confirming that the readings closely align with the true levels of the analytes in the sample as shown in Table 2.

The elevated recovery rates, generally around or surpassing 90%, imply that the colorimetric

Table 2. Recovery of spiked urinary biomarkers in synthetic urine utilizing colorimetric detection. This table displays the quantified concentrations of particular biomarkers (tyrosine, tryptophan, arginine, phenylalanine, cysteine, glucose, urea, creatinine, albumin, and uric acid) following the introduction of established standard amounts into artificial urine. The elevated recovery rates for all biomarkers demonstrate the dependability and precision of the colorimetric detection approach inside this matrix.

Sample with Artificial urine	Spiked concentration (mg\L)	Measured concentration (mg\L)	Recovery ratio* (%, *n = 3*)
Glucose	200	197.5	96.8± 0.07
Albumin	15	15.7	104.6± 0.05
Urea	800	784.28	98.03± 0.04
Uric acid	300	293	97.6± 0.02
Creatinine	200	210.4	105.2± 0.03
Tyrosine	20	21.11	105.5± 0.06
Tryptophan	25	24.8	99.2± 0.01
Arginine	50	47.71	95.42± 0.08
Cysteine	15	14.04	93.6± 0.07
Phenylalanine	20	20.18	100.9± 0.03

* Mean ± standard deviation (n = 3).

CC BY

assay is effective across many biomarkers, demonstrating the method's efficiency in extracting and quantifying the biomarkers inside the artificial urine matrix. This is especially important for clinical applications where precise and reliable biomarker measurement is crucial for diagnosing illnesses or monitoring health status. A high recovery rate does not ensure the elimination of potential biases; however, the results strongly suggest that the strategy reduces both systematic and random mistakes, thereby providing robust accuracy performance.

The uniformity of recovery rates among several biomarkers strengthens the method's reliability. Although the artificial urine matrix may not completely replicate the intricacies of authentic human urine, the lack of substantial influence from matrix constituents is demonstrated by the elevated recovery values. This indicates that the colorimetric detection method is adaptable and proficient in managing a wide range of biomarkers without experiencing significant matrix effects that

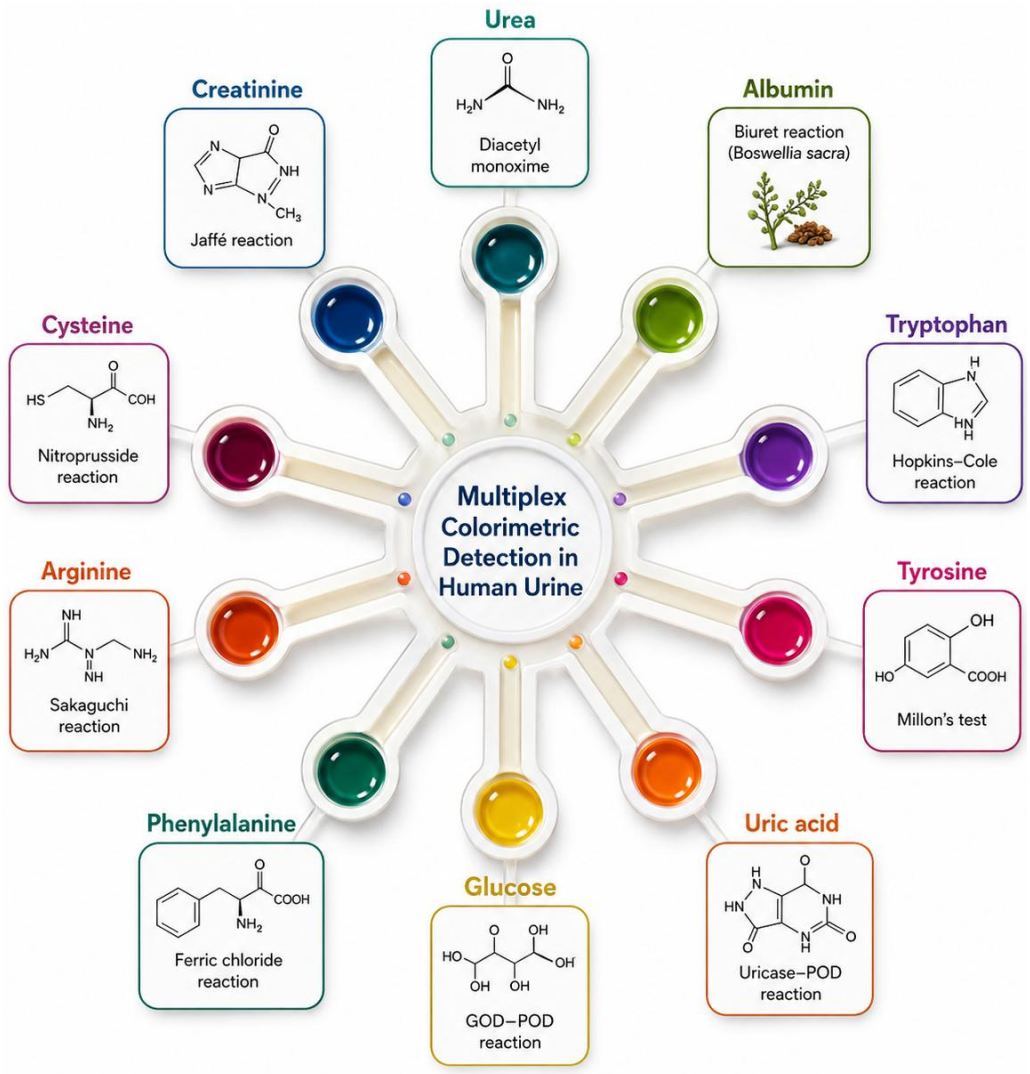

Fig. 8. Schematic illustration of the 3D-printed microfluidic apparatus for multiplex colorimetric analysis of urine biomarkers. The radial microchannel configuration facilitates the concurrent assessment of ten clinically pertinent biomarkers (tyrosine, tryptophan, arginine, phenylalanine, cysteine, glucose, urea, creatinine, albumin, and uric acid), with each branch incorporating a specific reagent that elicits a unique colorimetric reaction. The visual colour alterations illustrate the platform's capabilities for swift, selective, and simultaneous detection within a singular integrated device, underscoring its promise for point-of-care diagnostic applications.

CC BY

could compromise the results. Nevertheless, it is crucial to further authenticate these results using actual clinical urine samples to confirm that the recovery rates found in artificial urine accurately represent performance in more intricate biological matrices.

The outcomes of the recovery study indicate the possible application of this colorimetric assay in standard clinical diagnostics, especially for biomarkers commonly assessed in urine samples, including glucose, creatinine, and albumin. The capacity to attain elevated recovery rates across a diverse array of biomarkers illustrates the method's extensive application and appropriateness for non-invasive diagnostics. The elevated recovery rates indicate the assay's efficacy; nevertheless, investigating potential matrix effects in actual urine samples would be a prudent subsequent step to verify that the assay sustains high recovery rates and precision across diverse biological matrices.

Detection of Multiple Biomarkers in Human Urine

The concurrent identification of several biomarkers in human urine signifies a notable progress in clinical diagnostics, especially for early disease detection and thorough metabolic evaluation. Urine is a complex biological matrix comprising various metabolites and proteins, with quantities fluctuating based on healthy and pathological states, thus necessitating multiplexed investigation [40]. This study effectively utilized a microfluidic colorimetric platform for the quantitative detection of ten clinically significant biomarkers: tyrosine, tryptophan, arginine, phenylalanine, cysteine, glucose, urea, creatinine, albumin, and uric acid. Calibration curves for all analytes demonstrated exceptional linearity, with correlation values (R^2) exceeding 0.99, signifying good analytical dependability and precise quantification capacity (Table 1S). This exceptional linearity aligns with previous findings on microfluidic biosensors, which exhibit enhanced sensitivity and repeatability owing to meticulous regulation of microscale reaction conditions [41].

The established platform was further validated with 30 human urine samples, successfully quantifying the amounts of the examined biomarkers across normal, below-normal, and above-normal physiological ranges (Table 2S). The results indicated that the microfluidic device efficiently encompasses the clinically relevant concentration ranges of all ten biomarkers, indicating its suitability for real-sample analysis and possible diagnostic applications (Fig. 8). This feature is essential due to the heterogeneity in urine content among individuals and the necessity for precise detection throughout a broad dynamic range. The observed performance underscores the system's robustness in managing complex biological matrices without substantial loss of sensitivity or selectivity.

The suggested microfluidic technology presents several notable benefits over traditional analytical techniques, including high-performance liquid chromatography (HPLC), mass spectrometry, and routine spectrophotometric tests. Conventional techniques, although exceptionally precise, may necessitate advanced instrumentation, considerable sample preparation, and prolonged analysis durations, hence constraining their application in quick or point-of-care environments. Conversely, microfluidic technologies facilitate downsizing, decreased reagent and sample usage, expedited analysis, and the amalgamation of many tests inside a singular platform [40]. Recent advancements in microfluidic biosensors have shown their capacity for rapid, sensitive, and on-site detection with minimal user intervention, rendering them very appropriate for decentralized healthcare applications [42]. The incorporation of colorimetric detection streamlines the analytical procedure by enabling visual or image-based readouts without requiring intricate instrumentation.

The results indicate that the designed 3D microfluidic system provides a dependable, sensitive, and effective platform for multiplexed detection of urine biomarkers. Its superior analytical performance, along with operational ease and mobility, establishes it as a viable alternative to traditional laboratory procedures, with significant potential for use in clinical diagnostics, personalized medicine, and point-of-care testing.

CONCLUSION

This paper details the design, production, and application of a 3D-printed microfluidic system for multiplex colorimetric detection of clinically significant biomarkers in human urine. High-resolution 3D printing facilitated the swift production of consistent microfluidic chips with accurate channel geometry, while decreasing

CC BY

both manufacturing time and expenses relative to traditional fabrication methods. The radial microfluidic design incorporated several reaction zones on a single chip, facilitating concurrent analysis with little sample and reagent usage. The platform was assessed for the identification of ten urine biomarkers: tyrosine, tryptophan, arginine, phenylalanine, cysteine, glucose, urea, creatinine, albumin, and uric acid. Calibration curves exhibited exceptional linearity for all analytes ($R^2 > 0.99$), indicating dependable quantitative performance. Interference investigations demonstrated excellent selectivity in the presence of prevalent inorganic ions. An analysis of 30 human urine samples confirmed the device's efficacy in identifying biomarkers within clinically significant concentration ranges. In comparison to traditional analytical techniques, the suggested platform presents numerous practical benefits, such as expedited analysis, reduced reagent usage, minimal sample preparation, portability, and the simultaneous detection of various biomarkers on a single device. These attributes render it highly appropriate for point-of-care testing and decentralised clinical evaluation. This study illustrates that the amalgamation of 3D printing and microfluidic colorimetric sensing offers a straightforward, economical, and scalable method for multiplex urinalysis. The platform provides a basis for the advancement of lab-on-a-chip systems for clinical diagnostics and health surveillance.

CONFLICT OF INTEREST

The authors declare that there is no conflict of interests regarding the publication of this manuscript.

REFERENCES

1. Cheung AK, Chang TI, Cushman WC, Furth SL, Hou FF, Ix JH, et al. KDIGO 2021 Clinical Practice Guideline for the Management of Blood Pressure in Chronic Kidney Disease. Kidney Int. 2021;99(3):S1-S87.
2. Research Priorities for Kidney-Related Research—An Agenda to Advance Kidney Care: A Position Statement From the National Kidney Foundation. Am J Kidney Dis. 2022;79(2):141-152.
3. Catanese L, Siwy J, Mischak H, Wendt R, Beige J, Rupprecht H. Recent Advances in Urinary Peptide and Proteomic Biomarkers in Chronic Kidney Disease: A Systematic Review. Int J Mol Sci. 2023;24(11):9156.
4. Flagg ME, Bhandari SK, Pak KJ, Zhou H, Shaw SF, Shi JM, et al. Dialysis Transition Patterns of Chronic Kidney Disease Patients With and Without Heart Failure. Mayo Clin Proc. 2025;100(6):970-981.
5. Xiong L, Wu C, Chen S, Zhang Y, Wang L, Li Y, et al. Proteomics analysis reveals age-related proteins in the urine of chronic kidney disease patients. Frontiers in Medicine. 2025;11.
6. Makhammajanov Z, Kabayeva A, Auganova D, Tarlykov P, Bukasov R, Turebekov D, et al. Candidate protein biomarkers in chronic kidney disease: a proteomics study. Sci Rep. 2024;14(1).
7. Kopple JD, Jones M, Fukuda S, Swendseid ME. Amino acid and protein metabolism in renal failure. The American Journal of Clinical Nutrition. 1978;31(9):1532-1540.
8. Li X, Zheng S, Wu G. Amino Acid Metabolism in the Kidneys: Nutritional and Physiological Significance. Advances in Experimental Medicine and Biology: Springer International Publishing; 2020. p. 71-95. http://dx.doi.org/10.1007/978-3-030-45328-2_5
9. He Q, Ye B, Li H, Pan Y, Du Y, Yang K. Analysis of potential biomarkers for diabetic kidney disease and non-diabetic kidney disease based on urinary metabolomics analysis. BMC Nephrol. 2025;26(1).
10. Aitekenov S, Gaipov A, Bukasov R. Review: Detection and quantification of proteins in human urine. Talanta. 2021;223:121718.
11. Duranton F, Lundin U, Gayrard N, Mischak H, Aparicio M, Mourad G, et al. Plasma and Urinary Amino Acid Metabolomic Profiling in Patients with Different Levels of Kidney Function. Clin J Am Soc Nephrol. 2014;9(1):37-45.
12. Wu J, Chen Y-d, Gu W. Urinary proteomics as a novel tool for biomarker discovery in kidney diseases. Journal of Zhejiang University SCIENCE B. 2010;11(4):227-237.
13. Namera A, Yashiki M, Nishida M, Kojima T. Direct extract derivatization for determination of amino acids in human urine by gas chromatography and mass spectrometry. J Chromatogr B. 2002;776(1):49-55.
14. Gushue JN. Principles and Applications of Gas Chromatography Quadrupole Time-of-Flight Mass Spectrometry. Comprehensive Analytical Chemistry: Elsevier; 2013. p. 255-270. http://dx.doi.org/10.1016/b978-0-444-62623-3.00011-3
15. Christou C, Gika HG, Raikos N, Theodoridis G. GC-MS analysis of organic acids in human urine in clinical settings: A study of derivatization and other analytical parameters. J Chromatogr B. 2014;964:195-201.
16. Advanced Techniques in Gas Chromatography–Mass Spectrometry (GC–MS–MS and GC–TOF–MS) for Environmental Chemistry: Elsevier; 2013.
17. Smolinska A, Pellacani S, Skawinski M, Durante C. On the road to automation: a comparative review on chemometric strategies for GC-MS data analysis. TrAC, Trends Anal Chem. 2025;190:118286.
18. Hussein J. Principles and Applications of High-Performance Liquid Chromatography (HPLC): A Review. Biomedical and Pharmacology Journal. 2025;18(2):1087-1091.
19. Phipps WS, Crossley E, Boriack R, Jones PM, Patel K. Quantitative amino acid analysis by liquid chromatography-tandem mass spectrometry using low cost derivatization and an automated liquid handler. JIMD Reports. 2019;51(1):62-69.
20. Abdu Hussen A. High-Performance Liquid Chromatography (HPLC): A review. Annals of Advances in Chemistry. 2022;6(1):010-020.
21. Ahmed R. High-Performance Liquid Chromatography (HPLC): Principles, Applications, Versatality, Efficiency, Innovation and Comparative Analysis in Modern Analytical

CC BY

Chemistry and In Pharmaceutical Sciences. MDPI AG; 2024. http://dx.doi.org/10.20944/preprints202409.0057.v1
22. Compositional Analysis of Nickel(II)-Aminopolycarboxylic Acids Using UV-Vis Spectrophotometry.
23. Werle J, Buresova K, Cepova J, Bjørklund G, Fortova M, Prusa R, et al. Spectrophotometric and chromatographic analysis of creatine:creatinine crystals in urine. Spectrochimica Acta Part A: Molecular and Biomolecular Spectroscopy. 2024;322:124689.
24. Albishri A, Al-aqbi ZT, Moker MH, Jebur NQ, Murad DMA. 3D Printed Microfluidic Device-Based Highly Sensitive and Selective Sensor for Detection of Human Albumin in Urine Samples. BioNanoScience. 2025;15(4).
25. Al-Aqbi ZT, Albishri A, Hussein FH, Albukhaty S, Sulaiman GM, Khalil KAA, et al. A new 3D printing milli-fluidic device with integrated nanojunction for on-site colorimetric analysis of iron in water and soil samples. Chinese Journal of Analytical Chemistry. 2025;53(1):100475.
26. Alaziz BA, Al-Shakban M, Al-aqbi ZT. Nanosensors-based integrated microfluidic devices for therapeutic drug monitorIng of fentanyl citrate, tramadol, and pethidine in blood plasma. Microfluid Nanofluid. 2025;29(12).
27. Al-aqbi ZT, Abdulsahib HT, Al-Doghachi FAJ. A Portable Microfluidic Device-Based Colorimetric Naked-Eye Sensors for Determination of Mercury and Arsenic Ions in River Water Samples. Plasmonics. 2024;19(6):3393-3414.
28. Al-aqbi ZT, Yap YC, Li F, Breadmore MC. Integrated Microfluidic Devices Fabricated in Poly (Methyl Methacrylate) (PMMA) for On-site Therapeutic Drug Monitoring of Aminoglycosides in Whole Blood. Biosensors. 2019;9(1):19.
29. Al-aqbi ZT, Abdulsahib HT, Al-Doghachi FAJ. Micro/nanofluidic device for tamsulosin therapeutic drug monitoring in patients with benign prostatic hyperplasia at point of care. Anal Sci. 2024;40(6):1101-1110.
30. Khane Y, Albukhaty S, Sulaiman GM, Fennich F, Bensalah B, Hafsi Z, et al. Fabrication, characterization and application of biocompatible nanocomposites: A review. Eur Polym J. 2024;214:113187.
31. Al-Harrasi A, Rehman NU, Khan AL, Al-Broumi M, Al-Amri I, Hussain J, et al. Chemical, molecular and structural studies of Boswellia species: β-Boswellic Aldehyde and 3-epi-11β-Dihydroxy BA as precursors in biosynthesis of boswellic acids. PLoS One. 2018;13(6):e0198666.
32. Mannino G, Occhipinti A, Maffei M. Quantitative Determination of 3-O-Acetyl-11-Keto-βBoswellic Acid (AKBA) and Other Boswellic Acids in Boswellia sacra Flueck (syn. B. carteri Birdw) and Boswellia serrata Roxb. Molecules. 2016;21(10):1329.
33. Sharaf Zeebaree SY, Sharaf Zeebaree AY, Haji Zebari OI, Sharaf Zebari AY. Sustainable fabrication, optical properties and rapid performance of bio-engineered copper nanoparticles in removal of toxic methylene blue dye in an aqueous medium. Current Research in Green and Sustainable Chemistry. 2021;4:100103.
34. Green Synthesis of Copper Nanoparticles Using Syzygium Cumin, Leaf Extract, Characterization and Antimicrobial Activity. Chemical Science Transactions. 2018;8(1).
35. Liu M, Zhang S, Zhang Z, Liu Z, Liu K, Gao C. Sulfite modification of platinum nanoparticles modulates electrocatalytic formic acid oxidation activity. Green Chem. 2020;22(17):5838-5844.
36. Review for "A review on green synthesis of silver nanoparticles (SNPs) using plant extracts: a multifaceted approach in photocatalysis, environmental remediation, and biomedicine". Royal Society of Chemistry (RSC); 2024. http://dx.doi.org/10.1039/d4ra07519f/v1/review1
37. Kumar S, Tripathy SK, Kaushik N. A Review on Green Synthesis of Copper Nanoparticles Using Plant Extracts: Methods, Characterization, and Applications. Pharmaceutical Nanotechnology. 2025;13.
38. Saha I, Karmakar P, Bhattacharya D. Fungi-Mediated Fabrication of Copper Nanoparticles and Copper Oxide Nanoparticles, Physical Characterization and Antimicrobial Activity. Mycosynthesis of Nanomaterials: CRC Press; 2023. p. 112-125. http://dx.doi.org/10.1201/9781003327387-7
39. Mulvaney P. Zeta Potential and Colloid Reaction Kinetics. Nanoparticles and Nanostructured Films: Wiley; 1998. p. 275-306. http://dx.doi.org/10.1002/9783527612079.ch12
40. Sequeira-Antunes B, Ferreira HA. Urinary Biomarkers and Point-of-Care Urinalysis Devices for Early Diagnosis and Management of Disease: A Review. Biomedicines. 2023;11(4):1051.
41. Liu Z, Zhou Y, Lu J, Gong T, Ibáñez E, Cifuentes A, et al. Microfluidic biosensors for biomarker detection in body fluids: a key approach for early cancer diagnosis. Biomarker Research. 2024;12(1).
42. Chen S-J, Lu S-Y, Tseng C-C, Huang K-H, Chen T-L, Fu L-M. Rapid Microfluidic Immuno-Biosensor Detection System for the Point-of-Care Determination of High-Sensitivity Urinary C-Reactive Protein. Biosensors. 2024;14(6):283.

CC BY